



Hantzsch synthesis of 1,4-dihydropyridine derivatives over ZnO/ZrO₂ catalyst under solvent free condition

Prasad Sunkara, M Keshavulu, Veerasomaiah Puppala, P Vijay Kumar & Manohar Basude*

Department of Chemistry, Osmania University, Hyderabad, India

*E-mail: manoharbasude41@gmail.com

Received 13 March 2021; revised and accepted 26 July 2021

Hantzsch synthesis of 1,4-dihydropyridine derivatives is accomplished using novel and efficient ZnO/ZrO₂ catalyst. The catalysts prepared by facile precipitation and wet impregnation method have been characterized by using techniques like XRD, SEM, EDS, UV-diffuse reflectance spectra, FTIR, XPS, BET surface area. Ex situ Pyridine absorption FTIR spectroscopy is used to determine the Bronsted and Lewis acidic sites. Enhanced activity of the zirconia supported zinc catalyst is attributed to tetragonal phase, more acidic sites and high surface area of the catalyst. The products attained in good to excellent yields in short duration under solvent free condition, minimizing the disposal problem and energy dissipation. The catalyst can be reused umpteen times without significant loss in activity.

Keywords: Hantzsch synthesis, Zirconia supported zinc, Tetragonal phase, Solvent free condition, 1,4-Dihydropyridines

In recent times enormous interest is generated in synthesis of valuable heterocyclic scaffolds like 1,4-dihydropyridine derivatives due to their presence in several drugs, pharmaceuticals and natural products. 1,4-dihydropyridines exhibit significant biological activities such as anti-depression, anti-anxiety, analgesic, anti-tumor, hypnotic, vasodilating, bronchodilating and anti-inflammatory in addition to their use in the treatment of cardiovascular diseases as calcium channel blockers are synthesized effectively using Hantzsch reaction¹⁻⁴. This reaction has helped in building the important skeleton present in the prominent and clinically proven molecules such as Amlodipine, Nifedipine, Felodipine, Isradipine and Nicardipine⁵⁻⁷.

The potential advantage of one-pot multi-component reactions in organic synthesis is the atom economy with higher yields, reduction in number of steps with ease in work-up procedures⁸. Hantzsch synthesis is endowed with these characteristic features which further enable improvisation in terms of change of solvents, catalysts and even attributing the green features like solvent free condition and using water as solvent⁹⁻¹¹, considering its multifarious traits in contrast to regular organic solvents is attracting much attention¹²⁻¹⁴.

Organic synthesis utilizing conventional protocols suffers from the limitations like separation of the catalyst is difficult, prolonged reaction times, less

thermal stability of the catalyst at high temperatures, pollution of the products formed and use of toxic organic solvents¹⁵. To overcome the difficulties encountered in conventional protocols of organic synthesis the focus of the research is shifted to the heterogeneous catalysts¹⁶⁻¹⁸. Currently heterogeneous catalysts have come into prominence due to ease of separation, recovery, recyclability and use of small amount of the catalyst. In the last decade number of protocols and innumerable heterogeneous catalysts were developed for the synthesis of 1,4-dihydropyridine derivatives¹⁹⁻³³.

Zirconia (ZrO₂) has been extensively explored as catalyst support due to its acid-base bi-functional nature, hardness and thermal stability. ZrO₂ functions as catalyst in organic synthesis and transformation both in the form of single oxide and combined oxide³⁴. Sulphated zirconia and transition metal promoted sulphated zirconia catalyst is used for various organic reactions^{35,36}, in acetalization of glycerol³⁷, dealkylation of cumene and ethanol conversion³⁸. Catalytic activity of zirconia is based on presence of Bronsted and Lewis acid sites on the surface. The catalysts will become more promising on increasing surface acidity. The addition of transition metal atom into zirconia enhances the surface acidity and thermal stability of the combined oxide than the individual component oxide thereby increasing the catalytic performance^{39,40}. In our

quest to develop novel and efficient catalyst for environmentally benign protocol of Hantzsch synthesis of 1,4-dihydropyridines we have focused our attention on synthesis and characterization of zirconia and zirconia supported zinc oxide catalyst. Our present catalytic studies revealed that zirconia supported zinc oxide catalyst are promising for Hantzsch synthesis of 1,4-dihydropyridines. Selective products are obtained in high yield, short duration and environmentally benign conditions.

Materials and Methods

Catalyst preparation

Zirconium oxychloride octahydrate of quantity 10 g is added to 100 mL double distilled water. The resulting solution was made slightly alkaline by adding 5 N ammonia solution drop-wise under continuous stirring on a magnetic stirrer and resulting zirconium hydroxide collected free from ammonia on treatment with deionised water. The zirconium hydroxide obtained dried in an oven at 150 °C for 24 h was powdered and calcined at 600 °C for about 6 h. In preparation of 5% ZnO/ZrO₂, 0.839 g of zinc acetate dihydrate was dissolved in 10 mL of deionized water, and 5 g of zirconium hydroxide was added to it. Water was vapourized on water bath by continuous stirring. The resulting mixture was calcined at 600 °C for 6 h. Other catalysts were also prepared in a similar way using required metal salts.

Catalyst characterization

XRD 7000 Shimadzu instrument was used to record the powder X-ray diffraction patterns of samples using nickel filtered CuK_α radiation. The scattered intensity data is in the scanning range from 10° to 80° at a scan speed of 2.0 (deg/min), sampling pitch 0.02° and preset time 60 s. The average crystallite size of the particle is determined using Debye-Scherrer equation. Hitachi model SEM-EDS S3700N scanning electron microscopy at an applied voltage of 15.0 kV was used for scanning electron microscope (SEM)

investigations. BRUKER OPTICS model: TENSOR 27 spectrometer was used to record FTIR spectra of the catalyst at ambient conditions. The spectra were scanned using self-supporting KBr pellets containing the catalyst samples. UV-visible spectrophotometer (V650, JASCO) in the range 200–800 nm was used for UV-visible diffuse reflectance spectra (DRS) measurements. BaSO₄ was used as the reflectance standard. Nitrogen adsorption determined Brunauer-Emmett-Teller (BET) surface areas at -196 °C on a Quanta chrome autosorb automated gas sorption system. The X-ray photoelectron spectroscopic (XPS) images were recorded on a Shimadzu 3140 X-ray photoelectron spectrometer through excitation energy of 1253.6 eV (Mg Ka) and with 80 eV energy. The activity of the catalyst was tested according to the following general experimental procedure.

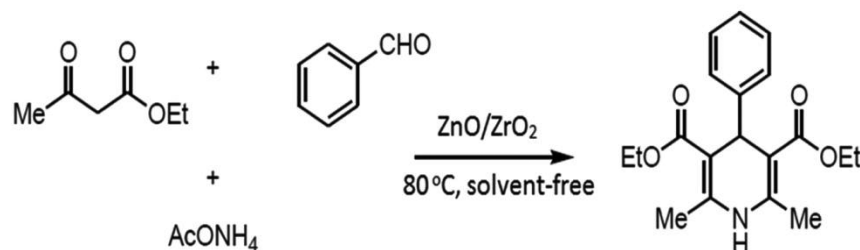
Catalytic activity test-Hantzsch reaction

In a 25 mL round bottomed flask containing 0.1 mol% of ZnO/ZrO₂, a mixture of aromatic aldehyde (10 mmol), ethyl acetoacetate (20 mmol) and ammonium acetate (15 mmol) were added. The reaction was tested under solvent free condition at 80 °C temperature. The progress of the reaction was monitored by TLC. The reaction mixture was dissolved in ethanol once the reaction is over and by filtration, the catalyst was separated. The products formed were purified and recrystallized from ethanol. Isolated yields of the products formed were determined. The reaction path way is given in Scheme 1. The products formed were determined using IR and NMR and the spectral data of the products were compared with the data of the compounds already available. Spectral data of the compounds is presented in Supplementary Data.

Results and Discussion

XRD analysis

The XRD patterns of the calcined samples of ZrO₂ and ZnO/ZrO₂ in the range of 2θ values 10°- 80° are



Scheme 1 — Hantzsch protocol for synthesis of 1,4-dihydropyridine derivatives

shown in Fig. 1. The simple ZrO₂ showed mixed phase such as monoclinic and tetragonal with some of the significant 2θ values 27.83, 29.85, 31.18, 33.91, 40.44, 49.99, 55.19, and 59.96°. Whereas the XRD pattern of ZnO modified ZrO₂ exhibit tetragonal phase with 2θ values 29.91, 34.81, 50.16 and 59.96°. The presence of percentage of tetragonal phase and monoclinic phase depends on the method of preparation, surface modification by ionic species, critical crystallite size, dopants creating oxygen ion vacancy and the occurrence of phase stabilizer either in the bulk or at the surface will affect the selective stabilization of the tetragonal phase of ZrO₂^{36,38}. A direct correlation is observed between crystallite size and the amount of tetragonal phase. The exclusive formation of tetragonal phase on the addition of a foreign element to ZrO₂ lattice can be attributed to the reduced grain boundary area between two zirconium atoms present side by side. This is due to surface modification occurred on introducing ionic species will prevent the transition from tetragonal phase to monoclinic phase. In accordance to this, the ZrO₂ crystal structure was significantly influenced due to the incorporation of Zn into ZrO₂ lattice, and tetragonal phase of ZrO₂ is formed from the monoclinic phase of ZrO₂ and stabilized on the addition of 5 wt% Zn²⁺. The diffraction peaks of crystalline ZnO species are not observed in the composite oxide, which may be due to the effective interaction of Zn ions with surface hydroxyl groups. The surface hydroxyl groups were not destroyed even after the calcination of the sample at 600 °C. This probably indicates ZnO species is well dispersed in the ZrO₂ matrix. In the current study, stabilization of

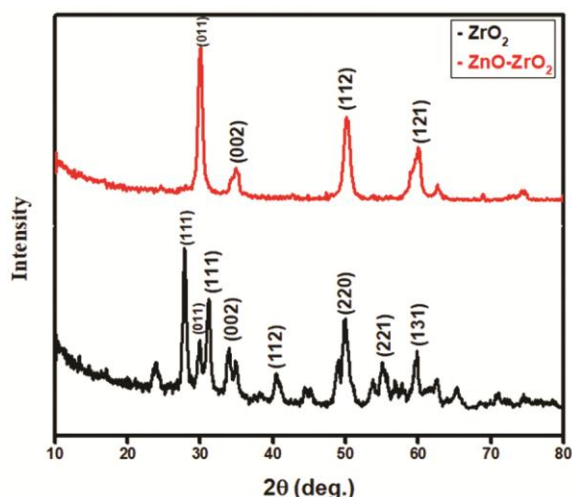


Fig. 1 — XRD patterns of pure ZrO₂ and ZnO/ZrO₂

the tetragonal phase of zirconia can be attributed to calcination at 600 °C and the existence of dopants such as Zn²⁺ ions in the ZrO₂ lattice which creates oxygen ion vacancy in the crystal lattice of ZrO₂ which in turn supports in the stabilization of the tetragonal phase. Average crystallite size calculated using Scherrer's formula for ZrO₂ and zinc promoted ZrO₂, where ZnO/ZrO₂ exhibits decrease in crystallite size and increase in surface area is attributed to the transformation of monoclinic phase to tetragonal phase. Our outcomes are in agreement with the literature data. The results are presented in Table 1.

FT-IR analysis

The FTIR spectra of both ZrO₂ and Zn promoted ZrO₂ samples are shown in the Fig. 2. In Fig. 2a the absorption bands appear at 348, 418, 490, 576, 664 and 740 cm⁻¹ are characteristic vibrations of Zr-O stretching and Zr-O-Zr asymmetric stretching of the crystalline ZrO₂ among which the bands at 576 cm⁻¹ and 740 cm⁻¹ are characteristic bands of monoclinic ZrO₂ whereas 490 and 664 cm⁻¹ are of tetragonal ZrO₂. The existence of these bands specifies the formation of crystalline ZrO₂ phase⁴¹. The peaks at 1531 and 1637 cm⁻¹ are recognized to symmetric and asymmetric vibrations of C=O bonds, respectively. The absorption peak at 2352 cm⁻¹ is due to the absorbed atmospheric CO₂ by metallic cations. The peaks in the range of 3600 to 3900 cm⁻¹ are attributed to water molecules absorbed by ZrO₂.

Fig. 2b shows the FTIR spectrum of Zn modified ZrO₂. The characteristic peaks of monoclinic phase of ZrO₂ at 576 cm⁻¹ and 740 cm⁻¹ disappear in Zn promoted ZrO₂. Here ZnO is present in highly dispersed state on ZrO₂ due to maximum consumption of the hydroxyl groups leading to the stabilization of the tetragonal phase and the absorption bands appearing at 457, and 670 cm⁻¹ are assigned to the t-ZrO₂ phase which was stabilized by impregnation of Zn into the ZrO₂ lattice. It is noteworthy that the peaks corresponding to Zn-O vibration are not observed in ZrO₂ supported Zn catalyst is consistent with XRD results.

Fig. 2c shows the pyridine absorbed FTIR spectra of ZrO₂ and Zn modified ZrO₂. Ex situ pyridine absorption FTIR spectroscopy is used to determine

Table 1 — Comparison of the crystallite size and surface area of the catalysts

Catalyst	Crystallite size (nm)	Surface area (m ² /g)
ZrO ₂	17.82	6.0
ZnO/ZrO ₂	15.6	43.195

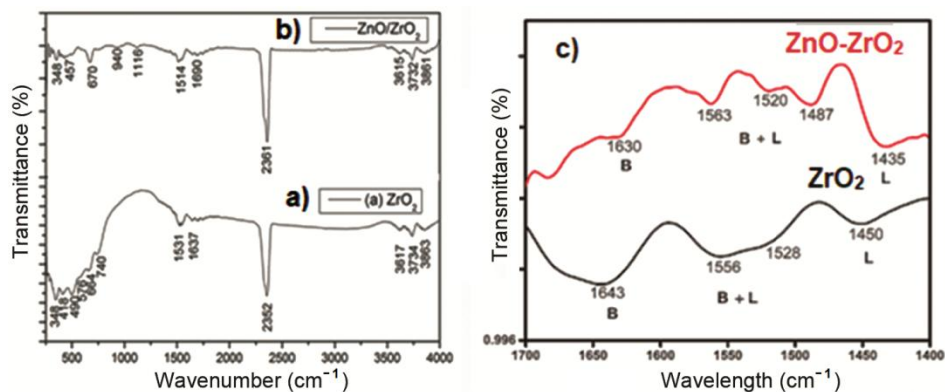


Fig. 2 — FTIR spectra of (a) pure ZrO_2 , (b) ZnO/ZrO_2 , (c) pyridine adsorbed FTIR spectra of pure ZrO_2 and ZnO/ZrO_2

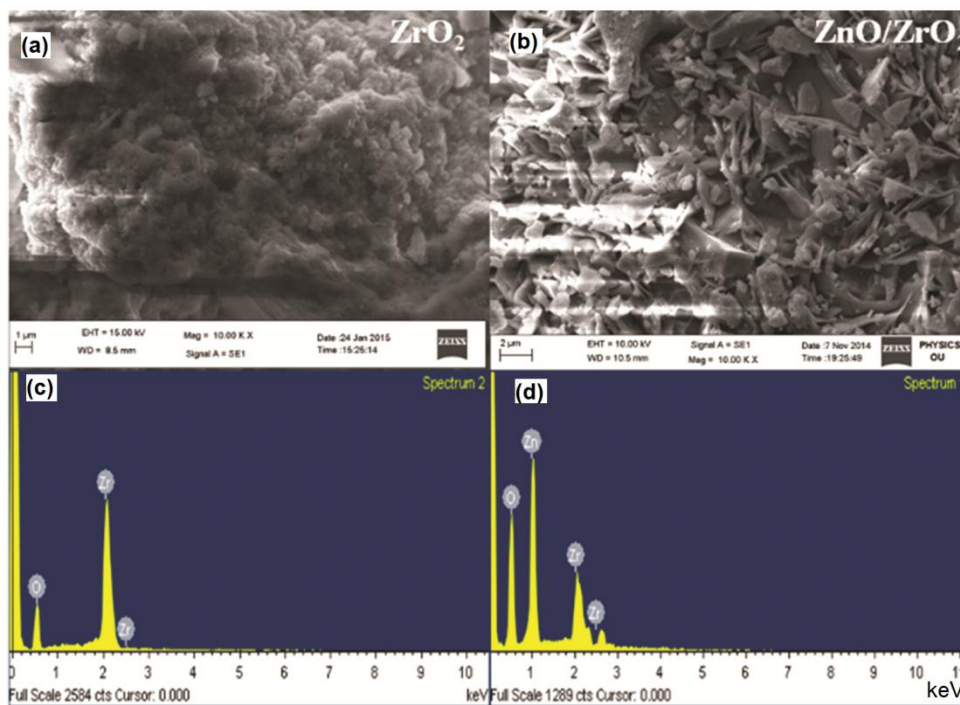


Fig. 3 — (a) SEM image of pure ZrO_2 (b) SEM image of ZnO/ZrO_2 and (c) EDS images of pure ZrO_2 and ZnO/ZrO_2

the Bronsted and Lewis acidic sites. The as synthesized samples were saturated with pyridine and dried at $150\text{ }^\circ\text{C}$ for 6 h prior to the FTIR analysis. ZrO_2 exhibited vibration bands at 1450, 1528, 1556 and 1645 cm^{-1} . The vibration band at 1450 cm^{-1} can be assigned to Lewis acidic sites where as vibration band at 1645 cm^{-1} is assigned to Bronsted acidic sites and vibration band at 1528 and 1556 cm^{-1} is due to both Lewis and Bronsted acidic sites. In ZrO_2 supported Zn sample vibration bands observed at 1435, 1487, 1520, 1563 and 1630 cm^{-1} . The vibration band at 1435 cm^{-1} corresponds to Lewis acidic site, the band at 1487 cm^{-1} is assigned to combination of Bronsted and Lewis acidic sites. The vibration bands

at 1520, 1563 and 1630 cm^{-1} are assigned to Bronsted acidic sites. Lewis acidity is more prominent in Zn promoted ZrO_2 catalyst is responsible for higher catalytic activity. The results are consistent with the literature data^{41,42}.

SEM and EDS analysis

Scanning electron microscope images of pure ZrO_2 and Zn modified ZrO_2 along with energy dispersive spectra (EDS) are shown in Fig. 3. The shape of the ZrO_2 is granular (Fig. 3a) and zinc modified ZrO_2 particles are flake like shape (Fig. 3b). The EDS of pure ZrO_2 (Fig. 3c) shows only Zr and O elements whereas the EDS of Zn modified ZrO_2 shows only Zn,

Zr and O elements in their stoichiometric ratio (Fig. 3d). We did not see the presence of any foreign element in the compounds.

UV-visible diffused reflectance spectra

The vibrational structure of all the three polymorphs of ZrO₂ is similar except small difference in band frequencies and intensities deduces difference in distribution of Zr⁴⁺ on the surface and bulk of ZrO₂. Band gap energy calculated for all the polymorphs is m-ZrO₂ 3.25 eV, t-ZrO₂ 3.58 eV and c-ZrO₂ 4.33 eV⁴². The UV-visible DRS of the pure ZrO₂ and ZnO/ZrO₂ recorded in the range 200–800 nm are shown in Fig 4. ZrO₂ exhibits an interband transition in the UV region of the spectrum as it is a direct band gap insulator. The differential plot of DRS of pure ZrO₂ exhibits two bands at 241.7 nm, 379.8 nm and the spectrum of zinc modified ZrO₂ exhibits two bands at 237.8 nm and 348.6 nm. The characteristic bands for ZrO₂ are generally observed at 240 nm. The results are in agreement with literature data. In ZrO₂, two bands observed are due to two band to band transitions. The bands observed correspond to presence of tetrahedral Zr⁴⁺ and charge transfer transition of O 2p electron from valence band to conduction band of Zr 4d. For the region above 400 nm up to 800 nm, no strong absorption bands were noted. From the spectra, it is clear that the shifting of the wavelength of absorption bands towards shorter wavelength upon doping of Zn into the ZrO₂. Band gap energy calculated for pure ZrO₂ is found to be 3.26 eV and 3.56 eV for Zn promoted ZrO₂. The band gap energy observed for pure ZrO₂ exactly coincides with monoclinic ZrO₂ and band gap observed for Zn promoted ZrO₂

coincides with tetragonal ZrO₂. In Zn modified ZrO₂ formation of the tetragonal phase is confirmed and the results are consistent with the IR and XRD results.

XPS studies

XPS analysis of the synthesized catalysts ZrO₂ and Zn-ZrO₂ was performed for understanding the oxidation states and chemical environment of the samples. Zr (3d) and oxygen (1s) core level XPS spectra of the sample ZrO₂ is given in Fig 5a. O (1s) photoelectron transition diagram of ZrO₂ exhibited a single peak at 530.1 eV binding energy. XPS spectra

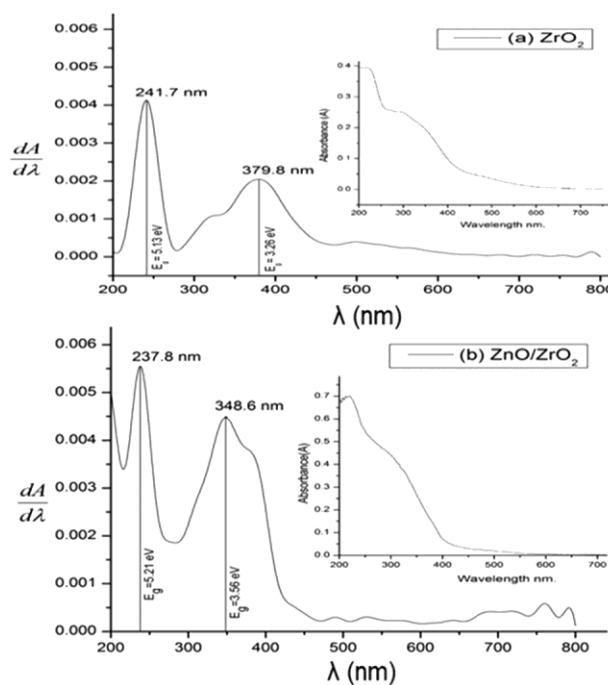


Fig. 4 — The UV-visible diffused reflectance spectra of (a) pure ZrO₂ and (b) ZnO/ZrO₂

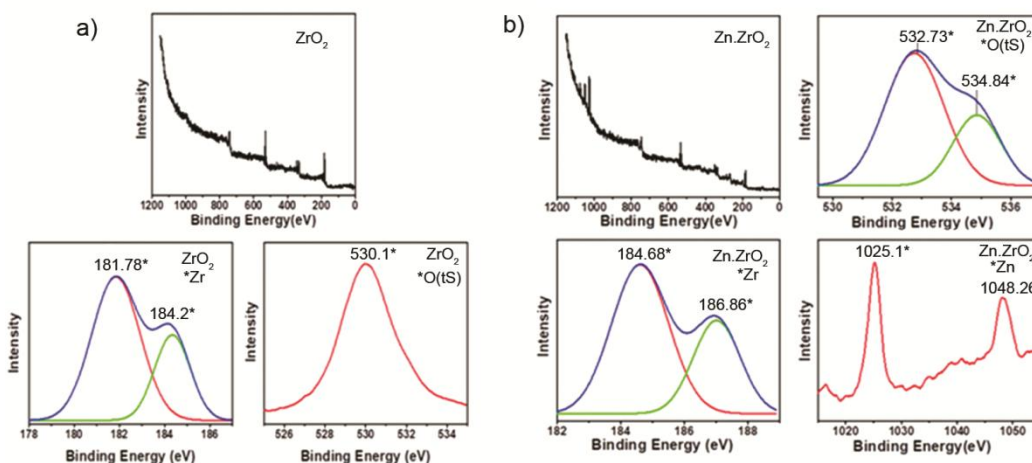


Fig. 5 — XPS results of (a) pure ZrO₂ and (b) ZnO/ZrO₂

of the sample Zn-ZrO₂ is given in Fig 5b. O 1s core level XPS spectra of the sample exhibits one peak at 532.73 eV and a shoulder at 534.84 eV. In metal oxides binding energy of O 1s is ≤ 531 eV and binding energy for hydroxide O 1s is ≥ 531 eV. In ZrO₂, peak at 530.1 eV is attributed to Zr-O-Zr bond. In Zn-ZrO₂ peak at 532.73 eV and 534.84 eV is ascribed to residual hydroxyl groups or surface oxygen bonded to zinc species.

Spin-orbit splitting of 3d component of Zr to Zr 3d_{5/2} and Zr 3d_{3/2} exhibit peaks at binding energy of 181.78 eV and 184.2 eV. The binding energy values indicate the presence of t-ZrO₂ and m-ZrO₂. The binding energy value for m-ZrO₂ is lower compared to t-ZrO₂ due to the holes created by the oxygen vacancies. The binding energy values specify the presence of Zr⁺⁴ ion whether it is m- or t- ZrO₂. In iron promoted ZrO₂ sample presence of higher amount of iron species shifts the binding energy values to lower side indicating that the presence of higher amount of iron species promotes reduction of the Zr oxidation state^{43,44}. In the present ZnO/ZrO₂ sample the binding energy values shift to higher side 184.68 eV and 186.86 eV may probably due to increase in surface oxygen species or surface hydroxyl species, respectively.

XPS spectra of ZnO/ZrO₂ exhibits spin orbit doublets formed by Zn 2p^{3/2} and Zn 2p^{1/2} electrons with binding energy values at 1025.1 eV and 1048.25 eV, respectively, indicates spin orbit splitting of 23 eV. The observed binding energy values are slightly higher side for Zn-O shows increase in surface concentration of oxygen species and hydroxyl species. The results presented agree with the literature data.

BET surface area

Dispersion of the layer of active component on the support surface prevents aggregation of the support particle, suppressing surface diffusion their by increasing surface area and thermal stability. Solid acids obtained by impregnation of Zr(OH)₄ with the active component possesses higher surface area compared to the catalyst obtained from ZrO₂. Surface area of the supported catalyst reaches maximum value at utmost dispersion capacity of the active component⁴⁵. The BET surface area of the catalysts determined using nitrogen physisorption technique and results are presented in Table 1. The BET surface area of pure ZrO₂ is 6 m²/g and for ZnO/ZrO₂ is 43.195 m²/g. There is a seven-fold increase in the

surface area of zirconia after incorporation of zinc into the zirconia lattice. In ZnO supported on Zr(OH)₄ dispersion of ZnO prevents transition of tetragonal to monoclinic phase and crystallization of ZrO₂. The increase in surface area of the catalyst is attributed to decrease in crystallite size in agreement with the results of XRD. The higher catalytic activity of zinc modified zirconia attributed to increasing in the surface area of the catalyst.

Catalytic activity

In preliminary investigation, the reaction conditions were optimized for Hantzsch synthesis of 1,4-dihydropyridine compounds employing several promoted ZrO₂ catalysts, varying temperature and in different reaction medium. The Hantzsch reaction between aldehyde, ethyl acetoacetate and ammonium acetate interestingly exhibited better results under a solvent free condition at 80 °C in the presence of different modified ZrO₂ catalysts. However, Zn modified ZrO₂ exhibited excellent catalytic activity for synthesis of 1,4-dihydropyridines (Scheme 1), in good to excellent yields in shorter reaction times relative to other catalysts and solvents. The results are as shown in the Table 2. However, phase stabilized ZrO₂ supported ZnO catalyst has shown more activity than ZrO₂, even though all the supported catalysts exhibit tetragonal phase. ZrO₂ possessing both acidic and basic sites observed to be less active towards the model reaction under solvent-free condition. Impregnation of Zn⁺² into ZrO₂ enhances the activity to a large extent than the other catalysts towards Hantzsch reaction reaching a maximum of 92% yield probably due to increase in acidity.

Reaction rate and yield of the products is influenced by the reaction temperature. Therefore, the influence of reaction temperature for the Hantzsch reaction was examined at different temperatures in the presence of ZrO₂ supported Zn catalyst under solvent-free condition and results are presented in Table 3. The increase in temperature completed the reaction in short duration with excellent yields of the products. The optimum temperature for this reaction to get better yields is 80 °C.

Table 2 — Comparison of activity of catalysts towards Hantzsch reaction under a solvent-free condition at 80 °C

Catalyst	Time (min)	Isolated yield (%)
Al ₂ O ₃ /ZrO ₂	90	91
Fe ₂ O ₃ /ZrO ₂	120	88
ZnO/ZrO ₂	45	92
ZrO ₂	135	90

Table 3 — Effect of temperature on Hantzsch reaction using benzaldehyde, ethyl acetoacetate and ammonium acetate in the presence of ZnO/ZrO₂

Temperature (°C)	Time (min)	Isolated yield (%)
60	70	89
80	45	92
100	30	85
120	20	87
140	12	83

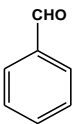
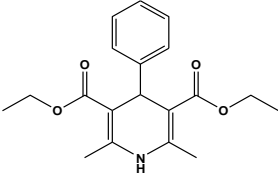
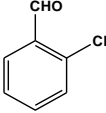
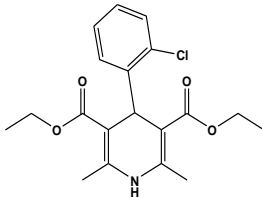
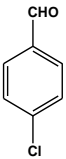
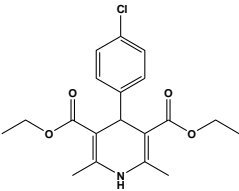
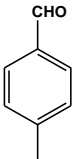
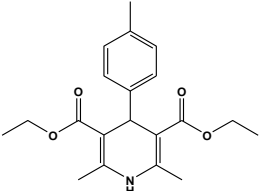
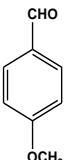
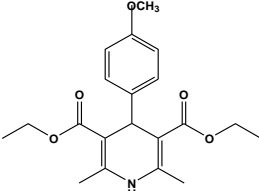
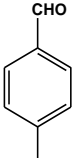
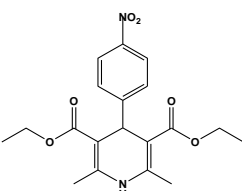
Table 4 — Effect of solvent on Hantzsch reaction using benzaldehyde, ethyl acetoacetate and ammonium acetate in the presence of ZnO/ZrO₂ at 80 °C

Solvent	Time (min)	Isolated yield (%)
DMSO	50	91
DMF	60	89
Acetonitrile	90	91
Ethanol	45	90
Water	60	86
Solvent-free	45	92

The Hantzsch reaction using benzaldehyde, ethyl acetoacetate and ammonium acetate in the presence of ZrO₂ supported ZnO catalyst in different solvents was monitored at 80 °C. The results are given in Table 4. The reaction in acetonitrile was slow while in ethanol was very fast. The activity was increased with increase in the solvent polarity except in water. Though water is highly polar, the activity of the catalyst for the reaction decreased in an aqueous medium. This may be due to the inhomogeneous dispersion of reactants in water. The activity of the catalyst for the reaction was same in ethanol as well as under solvent-free condition. In the environmentally friendly perspective, the solvent-free condition is preferred over any other solvent.

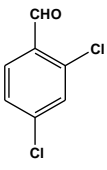
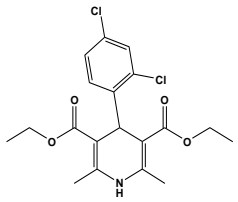
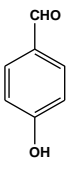
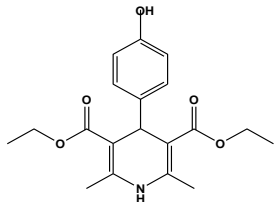
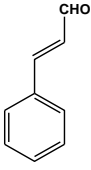
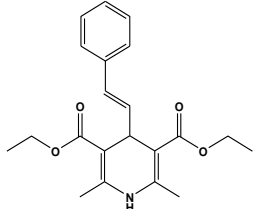
In Table 5, the reaction time and product yield for the Hantzsch reaction under solvent-free condition at 80 °C was presented. The environmentally benign catalyst ZnO/ZrO₂ examined using different aldehydes (aromatic, aliphatic and heterocyclic), ethyl acetoacetate and ammonium acetate in synthesis of dihydropyridine under solvent free condition affords excellent yields. All the reactions were completed in 25–65 min with yields above 90% (Table 5). To check the overview of the reaction several aldehydes with electron releasing groups and electron withdrawing groups were used in Hantzsch reaction. In comparison of reactivity of substituted aromatic aldehyde towards the Hantzsch reaction, the aldehyde with the electron withdrawing group is more reactive than the aldehyde with electron donating group. Among which the higher activity was observed for the reaction with

Table 5 — Hantzsch reaction in presence of ZnO/ZrO₂ at 80 °C under solvent-free condition

Reactant	Product	Time (min)	Isolated yield (%)
		45	92
		25	93
		60	92
		50	90
		65	91
		30	94

(Contd.)

Table 5 — Hantzsch reaction in presence of ZnO/ZrO₂ at 80 °C under solvent-free condition (Contd.)

Reactant	Product	Time (min)	Isolated yield (%)
		40	92
		60	94
		35	91

Reaction condition: 0.1 g of ZnO/ZrO₂ catalyst, a mixture of aromatic aldehyde (10 mmol), Ethyl acetoacetate (20 mmol) and Ammonium acetate (15 mmol), temperature 80 °C

2-chloro benzaldehyde and the reaction with 4-methoxy benzaldehyde is slow. From Table 5, it is clear that 2-chloro benzaldehyde is more reactive than 4-chloro benzaldehyde. It may probably due to chelating effect of zinc with chlorine and oxygen makes carbonyl carbon electron deficient facilitates easy attack by nucleophile generated from ethyl acetoacetate. Cinnamaldehyde shows greater reactivity towards Hantzsch reaction.

The catalyst was separated by simple filtration by dissolving the reaction mixture in a minimum amount of ethanol, washed several times with ethanol, dried and used for the same model reaction under solvent-free condition at 80 °C. There was no considerable change in yield up to four cycles for the Hantzsch reaction using different aldehydes under optimized conditions.

Conclusions

Zn modified ZrO₂ was prepared by wet impregnation of Zn⁺² on Zr(OH)₄ particles followed

by calcination at 600 °C. XRD pattern, UV-visible DRS and FT-IR data reveal that pure ZrO₂ crystallized in the mixture of monoclinic and tetragonal phase whereas Zn modified ZrO₂ stabilized to tetragonal phase. The catalytic activity of Zn modified ZrO₂ is more than the other catalysts towards Hantzsch reaction with good yields at 80 °C temperature. ZnO/ZrO₂ is more active because of the higher surface area due to its smaller particle size and higher acidic sites than ZrO₂. This is because of the creation of more active sites on the surface of the catalyst due to tetragonal phase, charge imbalance between metal ions and difference in redox potentials of metal ions. The catalyst is reusable for umpteen times.

Supplementary Data

Supplementary data associated with this article are available in the electronic form at [http://nopr.niscair.res.in/jinfo/ijca/IJCA_60A\(08\)1055-1063_SupplData.pdf](http://nopr.niscair.res.in/jinfo/ijca/IJCA_60A(08)1055-1063_SupplData.pdf).

Acknowledgement

Authors would like to thank UGC-SAP, DST-PURSE -II schemes, New Delhi.

References

- 1 Stout D M & Meyers A I, *Chem Rev*, 82 (1982) 223.
- 2 Shan R, Velazquez C & Knaus E E, *J Med Chem*, 47 (2004) 254.
- 3 Sawada Y, Kayakiri H, Abe Y, Mizutani T, Inamura N, Asano M, Hatori C, Aramori I, Oku T & Tanaka H, *J Med Chem*, 47 (2004) 2853.
- 4 Mannhold R, Jablonka B, Voigt W, Schoenafinger K & Schraven E, *Eur J Med Chem*, 27 (1992) 229.
- 5 Bossert F, Meyer H & Wehinger E, *Angew Chem Int Ed*, 20 (1981) 762.
- 6 Cosconati S, Marinelli L, Lavecchia A & Novellino E, *J Med Chem*, 50 (2007) 1504.
- 7 (a) Bossert F & Vater W, *US Patent No.* 3,485,847, Dec 23, 1969; (b) Neumann P, *US Patent No.* 4,466,972, Aug 21, 1984.
- 8 Dömling A & Ugi I, *Angew Chem Int Ed*, 39 (2000) 3168.
- 9 Hantzsch A, *Justus Liebigs Annalen der Chemie*, 215 (1882) 1.
- 10 Correa W H & Scott J L, *Green Chem*, 3 (2001) 296.
- 11 Sapkal S B, Shelke K F, Shingate B B & Shingare M S, *Tetrahedron Lett*, 50 (2009) 1754.
- 12 Kolvari E, Zolfigol M A & Peiravi M, *Green Chem Lett Rev*, 5 (2012) 155.
- 13 Li C J, *Chem Rev*, 93 (1993) 2023.
- 14 Kobayashi S & Manabe K, *Pure Appl Chem*, 72 (2000) 1373.
- 15 Gu Y, *Green Chem*, 14 (2012) 2091.
- 16 Ng E P, Lim G K, Khoo G L, Tan K H, Ooi B S, Adam F, Ling T C & Wong K L, *Mater Chem Phys*, 155 (2015) 30.

- 17 Cheong Y W, Wong K L, Ling T C & Ng E P, *Mater Express*, 8 (2018) 463.
- 18 Enache D I, Knight D W & Hutchings G J, *Catal Lett*, 103 (2005) 43.
- 19 Vahdat S M, Chekin F, Hatami M, Khavarpour M, Baghery S & Roshan-Kouhi Z, *Chinese J Catal*, 34 (2013) 758.
- 20 Saikia L, Dutta D & Dutta D K, *Catal Commun*, 19 (2012) 1.
- 21 Maheswara M, Siddaiah V, Damu G L V & Rao C V, *Arkivoc*, 2 (2006) 201.
- 22 Tajbakhsh M, Alaee E, Alinezhad H, Khanian M, Jahani F, Khaksar S, Rezaee P & Tajbakhsh M, *Chinese J Catal*, 33 (2012) 1517.
- 23 Kantam M L, Laha S, Yadav J & Srinivas P, *Synth Commun*, 39 (2009) 4100.
- 24 Safaei-Ghomi J, Ziarati A & Zahedi S, *J Chem Sci*, 124 (2012) 933.
- 25 Rao G D, Nagakalyan S & Prasad G, *RSC Adv*, 7 (2017) 3611.
- 26 Nasr-Esfahani M, Hoseini S J, Montazerzohori M, Mehrabi R & Nasrabadi H, *J Mol Catal A Chem*, 382 (2014) 99.
- 27 Karhale S, Bhenki C, Rashinkar G & Helavi V, *New J Chem*, 41 (2017) 5133.
- 28 Tiwari S K, Shivhare K N, Patel M K, Yadav V, Nazeef M & Siddiqui I, *Polycycl Aromat Compd*, (2020) 1.
- 29 Wu X Y, *Synth Commun*, 42 (2012) 454.
- 30 Kumar S, Sharma P, Kapoor K K & Hundal M S, *Tetrahedron*, 64 (2008) 536.
- 31 Bandyopadhyay D, Maldonado S & Banik B K, *Molecules*, 17 (2012) 2643.
- 32 Wang Q, Zhu M, Zhang H, Xu C, Dai B & Zhang J, *Catal Commun*, 120 (2019) 33.
- 33 Verma R, *Green Chem*, 1 (1999) 43.
- 34 Yamaguchi T, *Catal Today*, 20 (1994) 199.
- 35 Reddy B M & Patil M K, *Chem Rev*, 109 (2009) 2185.
- 36 Løften T, Gnep N S, Guisnet M & Blekkan E A, *Catal Today*, 100 (2005) 397.
- 37 Reddy P S, Sudarsanam P, Raju G & Reddy B M, *Catal Commun*, 11(2010) 1224.
- 38 El-Sharkawy E, Khder A & Ahmed A, *Microporous Mesoporous Mater*, 102 (2007) 128.
- 39 Samantaray S & Mishra B, *J Mol Catal A Chem*, 339 (2011) 92.
- 40 Maddila S, Rana S, Pagadala R, Kankala S, Maddila S & Jonnalagadda S B, *Catal Commun*, 61 (2015) 26.
- 41 Viswanadham B, Singh S, Friedrich H B & Mahomed A S, *S Afr J Chem*, 71 (2018) 62.
- 42 Ammaji S, Rao G S & Chary K V R, *Appl Petrochem Res*, 8 (2018) 107.
- 43 Basahel S, Ali T T, Narasimharao K, Bagabas A & Mokhtar M, *Mater Res Bull*, 47 (2012) 3463.
- 44 Basahel S N, Ali T T, Mokhtar M & Narasimharao K, *Nanoscale Res Lett*, 10 (2015) 73.
- 45 Zhao B Y, Xu X P, Ma H R, Sun D H & Gao J M, *Catal Lett* 45 (1997) 237.